Spectral shaping of Galileo signals in the presence of frequency offsets and multipath channels

Elena Simona Lohan, Abdelmonaem Lakhzouri, and Markku Renfors
Institute of Communications Engineering, Tampere University of Technology
P.O. Box 553, FIN-33101, Finland,
Tel: +358 3 3115 3915, Fax: +358 3 3115 3808
{*elena-simona.lohan, abdelmonaem.lakhzouri, markku.renfors*}*@tut.fi*

***Abstract*—Recently, the authors have proposed a new class of Binary-Offset-Carrier (BOC) modulation, namely the Double-BOC (DBOC) modulation which generalizes the main modulation types used in GPS and Galileo under a single, unified formula, and allows extra-flexibility in designing the suitable spectral shaping of future GNSS signals. The goal of this paper is to extend the previous analysis to multipath channels and to study the interference between various DBOC-modulated signals and the standard GPS signals in the presence of frequency offsets.**

Keywords: Double-Binary-Offset-Carrier (DBOC) modulation, Galileo, GPS, power spectral densities (PSD), spectral separation coefficients (SSC).

I. Introduction

The modulation type used for standard GPS signals, such as C/A and P(Y) codes, is the Binary Phase Shift Keying (BPSK) modulation [1]. The more recently proposed GPS and Galileo signals, such as GPS M-code, Open-Services (OS) and Publicly-Regulated-Services (PRS) signals, use a sine or cosine Binary-Offset-Carrier (BOC) modulation, described in [2], [3], [4], [5]. The three modulation types, namely BPSK, sine BOC (SinBOC) and cosine BOC (CosBOC), can be described by the help of a new, generalized class, introduced in [6] and denoted there as Double-BOC (DBOC) modulation class. DBOC modulation acts, indeed, as a double-stage-BOC modulation, and allows not only a general formulation of the current GPS and Galileo modulation types, but also more flexibility in shaping the desired signal spectrum and in achieving the target interference between signals sharing the same frequency bands.

The goal of this paper is to analyze the DBOC-modulated signals in the presence of multipath channels and frequency offsets and to show the additional benefits of using the DBOC class in the context of Galileo OS and PRS signals. By difference with previously defined modulation types (i.e., BPSK, SinBOC, and CosBOC), the DBOC modulation is fully described via three parameters: the BOC-modulation order of the first stage N_{BOC_1}, the BOC-modulation order of the second stage N_{BOC_2}, and the chip rate f_c. In the next section, we will briefly review the concept and main properties of DBOC modulation class. In section III, we introduce the theoretical derivations for multipath fading channels and frequency offsets. Section IV presents the simulation results and Section V summarizes the results of this paper.

This work was carried out in the project "Advanced Techniques for Mobile Positioning (MOT)" funded by the National Technology Agency of Finland (Tekes). This work is also partly supported by the Academy of Finland.

II. Double-BOC (DBOC) modulation

A DBOC-modulated wideband signal $z(t)$ can be seen as the convolution between a DBOC waveform $s_{DBOC}(t)$ and a data waveform, as follows:

$$z(t) = s_{DBOC}(t) \otimes \sum_{n=-\infty}^{+\infty} \sum_{k=1}^{S_F} b_n c_{k,n} \delta(t - nT_{sym} - kT_c), \quad (1)$$

where $\otimes$ is the convolution operator, b_n is the n-th complex data symbol (for the pilot channels, they may be assumed to be all equal to 1), T_{sym} is the symbol period, $c_{k,n}$ is the k-th chip corresponding to the n-th symbol, T_c is the chip period, S_F is the spreading factor ($S_F = T_{sym}/T_c$), $\delta(t)$ is the Dirac pulse, and $s_{DBOC}(t)$ is the DBOC waveform, defined as [6]:

$$s_{DBOC}(t) = p_{T_B}(t) \otimes \sum_{k=0}^{N_{BOC_2}-1} \sum_{i=0}^{N_{BOC_1}-1} (-1)^{i+k} \delta\Big(t - iT_{B_1} - kT_B\Big). \quad (2)$$

Above, N_{BOC_1} is the BOC-modulation order of the first stage, N_{BOC_2} is the BOC-modulation order of the second stage, T_{B_1} is the sub-chip interval after the first modulation stage: $T_{B_1} = T_c/N_{BOC_1}$, and $p_{T_B}(\cdot)$ is a rectangular pulse of amplitude 1 and support $T_B = \frac{T_c}{N_{BOC_1} N_{BOC_2}}$, where T_B is the sub-chip interval after the second modulation stage. The definition from eq. (2) of the DBOC waveform was inferred in [6] from the observation that CosBOC modulation is equivalent with a two-stage SinBOC modulation, in which the signal is first sine-BOC-modulated with a modulation order N_{BOC_1} (or, equivalently, a sub-carrier frequency $f_c N_{BOC_1}/2$, where $f_c = 1/T_c$ is the chip rate), and then, the sub-chip is further split into two parts (i.e., a second sine-BOC-modulation stage with $N_{BOC_2} = 2$ is applied). By extending the concept to $N_{BOC_2} > 2$, we got the expression of eq. (2).

From the point of view of implementation, we notice that eq. (2) is also equivalent with:

$$s_{DBOC}(t) = \begin{cases} sign\left(sin\left(\frac{N_{BOC_1} N_{BOC_2} \pi t}{T_c}\right)\right), \\ \text{if } N_{BOC_2} \text{ is odd}, \\ sign\left(\frac{sin\left(\frac{N_{BOC_1} N_{BOC_2} \pi t}{T_c}\right)}{sin\left(\frac{N_{BOC_1} \pi t}{T_c}\right)}\right), \\ \text{if } N_{BOC_2} \text{ is even}. \end{cases} \quad (3)$$

Therefore, for N_{BOC_2} odd, the DBOC signal is generated exactly as a sine-BOC signal, with subcarrier frequency $N_{BOC_1}N_{BOC_2}/T_c$, while for N_{BOC_2} even, we need two subcarrier frequencies: one equals to $N_{BOC_1}N_{BOC_2}/T_c$, and the other one equals to N_{BOC_1}/T_c. Hence, the generation of DBOC waveforms may be done via a quite straightforward implementation, by using some voltage controlled oscillators, similarly with what was explained in [7] for sine-BOC signals.

The DBOC modulation is completely defined via eq. (2) according to three parameters $(N_{BOC_1}, N_{BOC_2}, f_c)$. For various factors N_{BOC_2}, we also cover the BPSK, the SinBOC and the CosBOC cases (i.e., the main modulation types existing nowadays in GPS and Galileo systems):

$$\begin{cases} N_{BOC_1}=1, N_{BOC_2}=1 & \Rightarrow \text{DBOC} \equiv \text{BPSK} \\ N_{BOC_1}>1, N_{BOC_2}=1 & \Rightarrow \text{DBOC} \equiv \text{SinBOC} \\ N_{BOC_1}>1, N_{BOC_2}=2 & \Rightarrow \text{DBOC} \equiv \text{CosBOC} \\ N_{BOC_1}>1, N_{BOC_2}>2 & \Rightarrow \text{Higher-order DBOC} \end{cases} \quad (4)$$

The expression of eq. (2) allowed us to compute the normalized Power Spectral Density (PSD) $P_{DBOC}(f)$ of DBOC-modulation class in a straightforward and generic way, as shown in [6] (BPSK, SinBOC, and CosBOC are particular cases of the following expressions, as seen from eq. (4)):

1. If $N_{BOC_1}=$ odd and $N_{BOC_2}=$ odd :

$$P_{DBOC}(f)=\frac{1}{T_c}\left(\frac{sin(\pi fT_B)cos(\pi fT_c)}{\pi fcos(\pi fT_B)}\right)^2 \quad (5)$$

2. If $N_{BOC_1}=$ even and $N_{BOC_2}=$ odd :

$$P_{DBOC}(f)=\frac{1}{T_c}\left(\frac{sin(\pi fT_B)sin(\pi fT_c)}{\pi fcos(\pi fT_B)}\right)^2 \quad (6)$$

3. If $N_{BOC_1}=$ odd and $N_{BOC_2}=$ even :

$$P_{DBOC}(f)=\frac{1}{T_c}\left(\frac{sin(\pi fT_B)sin(\pi fT_{B_1})cos(\pi fT_c)}{\pi fcos(\pi fT_B)cos(\pi fT_{B_1})}\right)^2 \quad (7)$$

4. If $N_{BOC_1}=$ even and $N_{BOC_2}=$ even :

$$P_{DBOC}(f)=\frac{1}{T_c}\left(\frac{sin(\pi fT_B)sin(\pi fT_{B_1})sin(\pi fT_c)}{\pi fcos(\pi fT_B)cos(\pi fT_{B_1})}\right)^2 \quad (8)$$

where $T_{B_1}=\frac{T_c}{N_{BOC_1}}$ and $T_B=\frac{T_c}{N_{BOC_1}N_{BOC_2}}$ are the subchip intervals after the first and, respectively, the second BOC-modulation stages.

In eqs. (5) to (8), the normalization was done with respect to the chip period T_c, or, equivalently, to the signal power over infinite bandwidth, similar to [2].

Fig. 1 shows the normalized PSD of several DBOC-modulated signals, for a chip frequency $f_c = 1.023$ MHz. The SinBOC in this figure corresponds to the classical case BOC$(1,1)$ [4]. The PSDs are given in dBW-Hz (P_{DBOC} [dBW-Hz]$\triangleq 10log_{10}P_{DBOC} - 60$). We remark that, when N_{BOC_2} modulation order increases, the signal main lobes move further towards the outer sides of the spectrum. This is also in accordance with the observations in [4], where it was noticed that the CosBOC modulation had the advantage that it concentrated more power on outer sides of spectrum compared to the SinBOC modulation of the same order. Hence, the interference with GPS signals could be reduced via increasing N_{BOC_2}, at the expense of a higher bandwidth (as seen in Fig. 1).

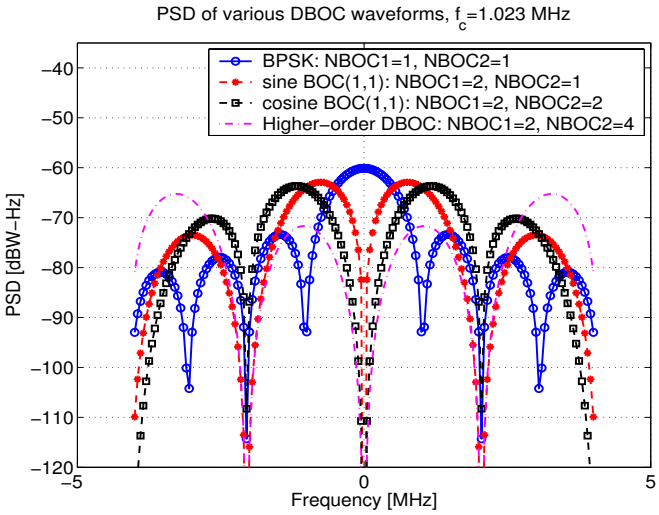

Fig. 1. Examples of PSDs for DBOC-modulated waveforms.

The autocorrelation function (ACF) of a DBOC waveform can also be easily derived based on eq. (2):

$$\mathcal{R}_{DBOC}(t) \triangleq s_{DBOC}(t) \otimes s_{DBOC}(t) = \Lambda(t) \otimes \sum_{k=0}^{N_{BOC_2}-1} \sum_{j=0}^{N_{BOC_2}-1} \sum_{i=0}^{N_{BOC_1}-1} \sum_{l=0}^{N_{BOC_1}-1} (-1)^{k+j+i+l} \times \delta(t - iT_{B_1} + lT_{B_1} - kT_B + jT_B), \quad (9)$$

where $\Lambda_{T_B}(t)$ is the triangular pulse of support $2T_B$, (i.e., the ACF of a rectangular pulse of support T_B). Eq. (9) allows us to compute, in a generic way, the ACF of a DBOC-modulated signal in the presence of multipath fading channels, as it will be shown in Section III.

The ACFs of several DBOC-modulated signals are shown in Fig. 2. We notice that, typically, the higher the N_{BOC_2} is, the smaller width of the main lobe we have (and hence, better resolution during delay tracking). On the other hand, due to an increased $N_{BOC_1}N_{BOC_2}$ product, the number of sidelobes within two-chips interval increases, thus increasing the ambiguities in the signal ACF, which might make the acquisition process more difficult [8].

III. Behaviour in the Presence of Multipath Fading Channels and Frequency Offsets

The baseband equivalent model of a DBOC-modulated signal $x(t)$ received over a fading multipath channel with additive Gaussian noise $\eta(t)$ is

$$y(t) = x(t) \otimes s_{DBOC}(t)e^{j2\pi f_o t} \otimes \varepsilon_{ch}(t) + \eta(t), \quad (10)$$

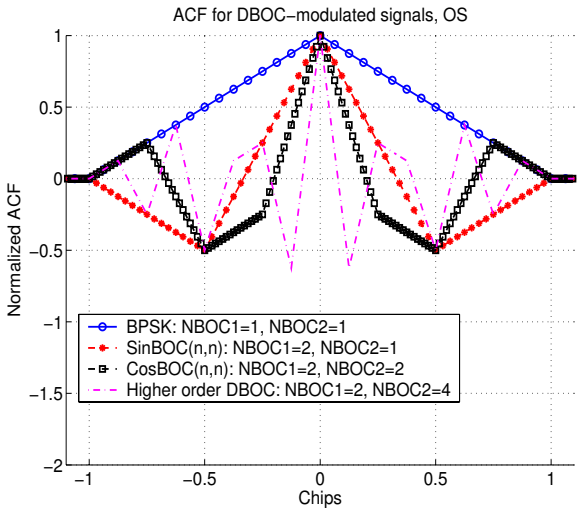

Fig. 2. Examples of the normalized ACFs of DBOC-modulated waveforms

where $x(t) = \sum_{n=-\infty}^{\infty} \sum_{k=1}^{S_F} b_n c_{k,n} \delta(t - nT_{sym} - kT_c)$ is the spread data sequence, f_o is the frequency offset with respect to the carrier frequency, and $\varepsilon_{ch}(t)$ is the channel impulse response:

$$\varepsilon_{ch}(t) = \sum_{l=1}^{L} \alpha_l \delta(t - \tau_l),$$

with α_l being the complex channel coefficients of l-th path, τ_l the corresponding multipath delays, and L the number of channel paths. If we assume that the signal and the noise are uncorrelated processes, the PSD of signal $y(t)$, conditional to the channel coefficients α_l and delays τ_l, can be derived from eq. (10) as:

$$P_y(f) = X_{PSD}(f) P_{DBOC}(f - f_o) \left| \sum_{l=1}^{L} \alpha_l e^{-j2\pi f \tau_l} \right|^2 + N_0, \quad (11)$$

where N_0 is the noise PSD in the considered bandwidth and $X_{PSD}(f)$ is the PSD of the spread data sequence, and $P_{DBOC}(f - f_o)$ is the PSD of the DBOC-modulated waveform (given in Section II, eqs. (5) to (8)) and centered at the frequency offset f_o. The unconditional PDF of $y(t)$ signal was computed in the simulations by averaging over several random channel realizations. A theoretical derivation of the PSD of a spread sequence $x(t)$ can be found in [9]. However, in what follows, we assume that the code chips and the data symbols are independent and that the code sequence has ideal autocorrelation properties, i.e., $\mathbf{E}(c_{k,n} c_{i,m}) = \delta(n-m)\delta(k-i)$. In this case, $X_{PSD}(f) = 1$.

The spectral separation coefficient (SSC) between two DBOC-modulated signals in the presence of multipath fading channels and frequency offsets, is defined similar with [2], [6]:

$$\kappa_{SSC} = \int_{-B_T/2}^{B_T/2} \widetilde{P}_{y_1}(f) \widetilde{P}_{y_2}(f) df, \quad (12)$$

where B_T is the complex receiver bandwidth over which the SSC is computed, $\widetilde{P}_{y_\upsilon}(f)$ is the PSD of the υ-th signal ($\upsilon = 1, 2$), normalized over bandwidth B_T: $\widetilde{P}_{y_\upsilon}(f) \triangleq P_{y_\upsilon}(f) / \left(\int_{-B_T/2}^{B_T/2} P_{y_\upsilon}(f) df \right)$, and $P_{y_\upsilon}(f)$ is given by eq. (11).

The SSC coefficients are useful measures of the interference between future Galileo signals and existing GPS signals (i.e., C/A code, M-code and P(Y)-code), as well as for the characterization of the self-interference [2], [6] .

In terms of the autocorrelation function, the ACF of the received signal, after the removal of data modulation and for zero-frequency offset is:

$$\mathcal{R}_y(t) \triangleq y \otimes y^{'}(t) = \sum_{l=1}^{L} \sum_{l_1=1}^{L} \alpha_l \alpha_{l_1}^{'} \mathcal{R}_{DBOC}(t - \tau_l + \tau_{l_1}) + N_0 \delta(t), \quad (13)$$

where the upper-script $^{'}$ stands for the conjugate and $\mathcal{R}_{DBOC}(t)$ is given in eq. (9).

IV. Simulation Results

In the simulations, we considered Rayleigh and Rician fading channels, with decaying power delay profiles, meaning that the relationship between the average path powers of two consecutive paths $P_l \triangleq E(|\alpha_l|^2)$ and $P_{l+1} \triangleq E(|\alpha_{l+1}|^2)$ was given by $P_{l+1} = P_l e^{-\mu(\tau_{l+1} - \tau_l)}$, where μ is the exponential-decaying coefficient (here, $\mu = 10^{-6} f_c$). The number of channel paths was assumed to be random and uniformly distributed between 1 and L_{max} (L_{max} is specified in the figures captions or labels). The maximum separation between successive paths was assumed to be 2 chips (however, the simulation results showed that this parameter has no impact on the results from the point of view of spectral properties of the DBOC signals).

Fig. 3 shows the SSC (mean and maximum or worst-case values) between various DBOC signals and the standard GPS signals. The average and the maximum values of SSC are computed over 5000 random channel realizations. The average values are plotted with continuous lines, and the worst-case values are plotted with dashed lines (this holds also for Fig. 4). Both desired and interfering signals are assumed to have a Rician distribution of the first path and Rayleigh distribution for successive paths (if any), and the channels of desired and interfering signals are modelled as explained above. Here, we assume that the maximum number of channel paths is the same for the desired and interfering signal, and this number is shown in the horizontal axis.

We see here that the channel profiles (the number of paths) have little impact on the SSC factors, fact which was also verified for Rayleigh-fading-first-path channels and for various other levels of Carrier-to-Noise Ratio (CNR). We also see that, when $N_{BOC_1} = 2$ as in Fig. 3, by increasing the modulation order of the second stage, we may decrease the spectral separation with C/A code. The spectral separation factors with the other GPS codes remain almost unchanged in this case. The difference between the worst-case and the average SSC values can be up to 3.5 dBW/Hz and it is slightly worst for C/A code and self-SSC factors than for SSC with P(Y) and M codes.

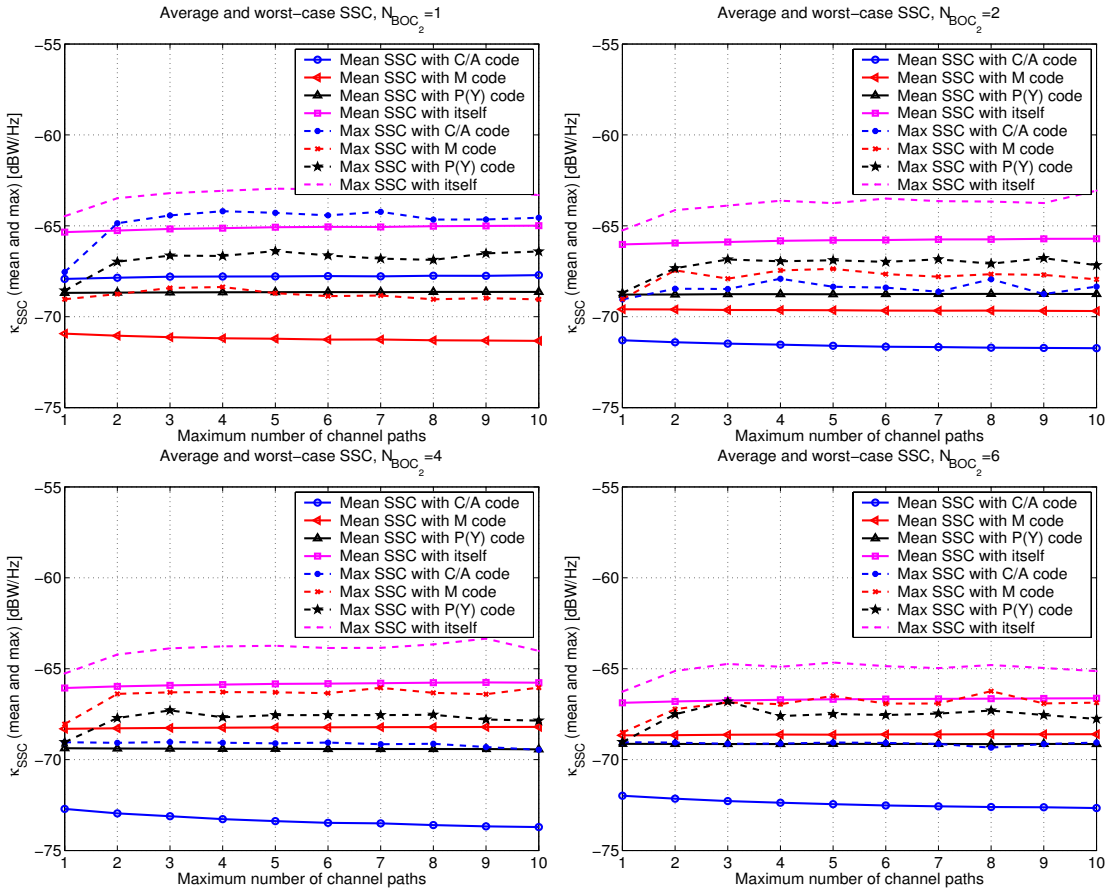

Fig. 3. Average spectral-separation coefficients for 4 DBOC signals in the presence of multipath fading channels: $N_{BOC_1} = 2$ (as for OS) and N_{BOC_2}=1, 2, 4, and 6, respectively. Zero frequency offset, CNR=45 dB-Hz.

The maximum Value of the Spectrum (MVS) and the Root Mean Square bandwidth (RMS BW) for various DBOC signals are shown in Fig. 4. For MVS and RMS BW, the definition of [2] was used. An increased number of paths means a higher level of interference, and therefore MVS value increases, as seen in the upper plot of Fig. 4. On the other hand, the RMS BW (and hence, the inverse of the variance of delay tracking process [10]) decreases very slowly with the increase in the number of paths. The best values for MVS and RMS BW (both the average and worst-case values) are achieved here with a higher-order DBOC modulation (i.e., $N_{BOC_2} = 4$). Therefore, increasing the second-stage modulation order may be beneficial in achieving better spectral properties.

Fig. 5 shows the average SSC coefficients for the interference between the current Galileo candidates and the GPS signals in the presence of multipath channels and frequency offsets. The multipath channels were having up to 4 paths, with power decay profiles and maximum separation between consecutive paths of 2 chips. Similar results have been obtained for all the studied channel profiles, as illustrated before (e.g., in Fig. 3), therefore the channel profile does not seem to affect the results in any significant way. On the other hand, the impact of the frequency offsets is much more significant, as seen in Fig. 5.

The candidate considered for OS services is SinBOC(1,1) (upper plot of Fig. 5) and the candidate for PRS services is CosBOC(15,2.5) (lower plot of Fig. 5). The channels were assumed to be Rician fading channels, with random number of paths and decaying power delay profile. Similar curves were obtained for other channel profiles as well. The receiver bandwidth was taken equal to $B_T = 8$ MHz for OS and $B_T = 40$ MHz for PRS [11].

We remark from Fig. 5 (upper plot) that the lowest $\kappa_{SSC,C/A\_code}$ for OS is obtained for about 4 MHz frequency offset between the SinBOC$(1,1)$ signal and the C/A code. Similarly, the lowest κ_{SSC,M_code} for OS is obtained for about 5.11 MHz frequency offset between the SinBOC$(1,1)$ signal and the M code. For PRS signals shown in the lower plot of Fig. 5, the smallest $\kappa_{SSC,C/A\_code}$ and κ_{SSC,M_code} coefficients occur at zero frequency offset between the CosBOC$(15,2.5)$ signal and the M-code.

V. Conclusions

This paper presents a new class of modulation for Galileo and modernized GPS signals, the Double-BOC modulation, in the presence of multipath fading channels and frequency offsets. The main properties of the DBOC family, namely the autocorrelation function and the power spectral densities, are derived analytically, in a generic framework, which allows a

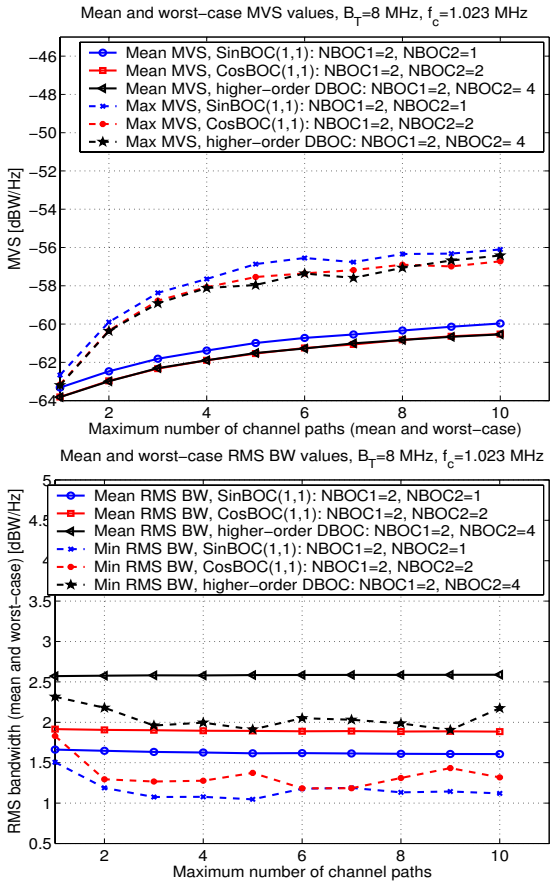

Fig. 4. Maximum value of the spectrum (upper plot) and RMS bandwidth (lower plot) for 3 DBOC signals in the presence of multipath fading channels. $B_T = 8$ MHz, $f_c = 1.023$ MHz, zero frequency offset, CNR=45 dB-Hz.

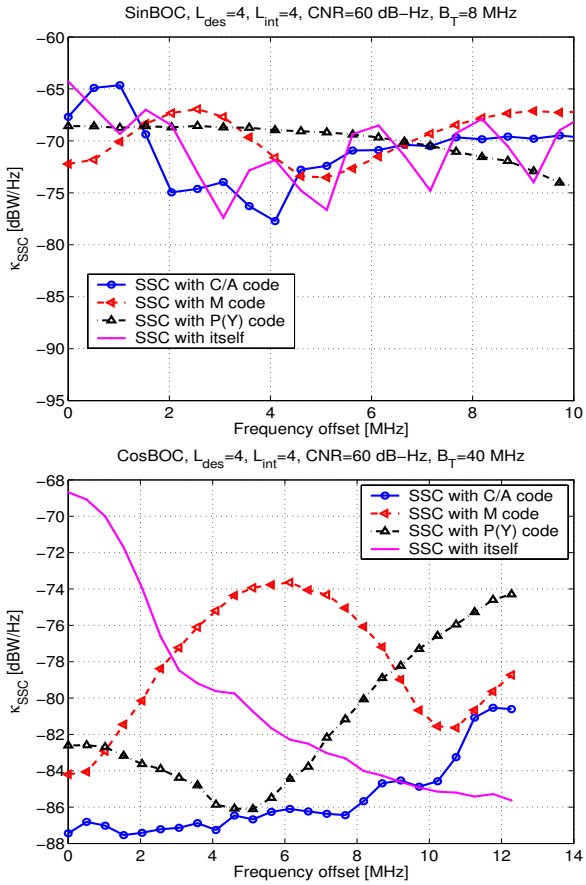

Fig. 5. SSC coefficients for the current OS (upper plot) and PRS (lower plot) Galileo candidates in the presence of multipath fading channels and frequency offsets. L_{des} is the maximum number of paths of the desired (DBOC) signal, L_{int} is the maximum number of paths of the interfering signal (i.e., GPS signals or another DBOC signal).

unified analysis of the existing BPSK, SinBOC and CosBOC modulation types. Simulation results are also shown in order to exemplify the potential use of DBOC modulation in the context of future satellite navigation systems. We also showed that, via the DBOC modulation, the spectral shaping can be made more flexible, due to the two modulation orders, N_{BOC_1} and N_{BOC_2} which control the power spectral density of the signal and its bandwidth consumption.

REFERENCES

[1] J. Betz and D. Goldstein, "Candidate Designs for an Additional Civil Signal in GPS Spectral Bands." MITRE Technical Papers, Jan 2002.

[2] J. Betz, "The Offset Carrier Modulation for GPS modernization," in *Proc. of ION Technical meeting*, pp. 639–648, 1999.

[3] B. Barker, J. Betz, J. Clark, J. Correia, J. Gillis, S. Lazar, K. Rehborn, and J. Straton, "Overview of the GPS M Code Signal," in *CDROM Proc. of NMT*, 2000.

[4] G. Hein, M. Irsigler, J. A. Rodriguez, and T. Pany, "Performance of Galileo L1 signal candidates," in *CDROM Proc. of European Navigation Conference GNSS*, May 2004.

[5] V. Heiries, D. Oviras, L. Ries, and V. Calmettes, "Analysis of non ambiguous BOC signal acquisition performance," in *CDROM Proc. of ION GNSS*, Sep 2004.

[6] E. Lohan, A. Lakhzouri, and M. Renfors, "A novel family of Binary-Offset-Carrier modulation techniques with applications in satellite navigation systems." Technical Report, Tampere University of Technology, ISBN 952-15-1348-9, ISSN 1459–4617, Apr 2005 (also submitted to Wiley International Journal of Wireless Comm. and Mobile Computing).

[7] L. Ries, F. Legrand, L. Lestarquit, W. Vigneau, and J. Issler, "Tracking and multipath performance assessments of BOC signals using a bit-level signal processing simulator," in *Proc. of ION-GPS2003*, (Portland, OR, US), pp. 1996–2009, Sep 2003.

[8] N. Martin, V. Leblond, G. Guillotel, and V. Heiries, "BOC(x,y) signal acquisition techniques and performances," in *Proc. of ION-GPS2003*, (Portland, OR, US), pp. 188–198, Sep 2003.

[9] N. Pronios and A. Polydoros, "On the power spectral density of certain digitally modulated signals with applications to code despreading," *IEEE Journal on Selected Areas in Comm.*, vol. 8, pp. 837–852, Jun 1990.

[10] J. Betz, "Design and Performance of Code Tracking for the GPS M Code Signal," in *CDROM Proc. of ION Meeting*, Sep 2000.

[11] J. A. Rodriguez, M. Irsigler, G. Hein, and T. Pany, "Combined Galileo/GPS frequency and signal performance analysis," in *CDROM Proc. of ION GNSS*, Sep 2004.